AAPS PharmSciTech, Vol. 15, No. 6, December 2014 (© 2014)
DOI: 10.1208/s12249-014-0179-7

Research Article

Comparative Study on the Suitability of Two Techniques for Measuring the Transfer of Lipophilic Drug Models from Lipid Nanoparticles to Lipophilic Acceptors

Mohamed Dawoud[1,2] and Fahima M. Hashem[1]

Received 3 April 2014; accepted 15 July 2014; published online 16 August 2014

Abstract. Due to their particle size in the submicrometer range, lipid nanoparticles are suitable for parenteral administration. In order to obtain information on their potential *in vivo* performance, a simple and effective *in vitro* assay to evaluate the drug release behavior of such particles is required. This study compares the use of different experimental setups for this purpose. Lipid nanoparticles from trimyristin which were loaded with fluorescent lipophilic drug models (a temoporfin and Nile red) were used as donor particles. The transfer of the two drug models to multilamellar vesicles (MLV) and emulsion droplets as lipophilic acceptor compartments was examined. The determination of the transferred substance was performed either after separation by centrifugation or by an *in situ* flow cytometric technique. The transfer of temoporfin was slow to the acceptor MLV and very rapid to the acceptor emulsion. With both acceptors, the transfer of temoporfin stopped at a concentration much lower than the theoretical equilibrium values. The transfer of the less lipophilic drug Nile red was very rapid to both acceptors with equilibrium concentrations close to the expected values. The transfer results of temoporfin especially to the acceptor MLV obtained with the two detection techniques were comparable while the centrifugation technique indicated an apparently higher Nile red transfer rate than the flow cytometric technique. Both techniques are equally suitable to study the transfer of temoporfin, while the flow cytometric technique is advantageous to measure the very rapid transfer of Nile red.

KEY WORDS: drug transfer; flow cytometry; lipid nanoparticles; liposomes; ultracentrifugation.

INTRODUCTION

Lipid nanoemulsions, which were introduced for the purpose of parenteral nutrition, are usually composed of fatty vegetable oils (*e.g.*, soybean oil) or medium chain triglycerides as the lipid phase. During recent years, it has been recognized that these systems may also be used as carriers for lipophilic drugs and several formulations have been commercialized (1–4). Advantages of nanoemulsions include toxicological safety and a high content of the lipid phase as well as the possibility of large-scale production by high-pressure homogenization. The possibility of controlled drug release from these lipid nanoemulsions is limited due to the liquid state of the carrier. For most drugs, a rapid release of the drug has to be expected (5–8). The use of solid lipids instead of liquid oils is a very attractive approach to achieve sustained drug release from nanoparticulate lipid carriers, because drug mobility in a solid lipid should be considerably lower compared with liquid oil. Although a decrease in drug mobility has indeed been observed in lipid dispersions containing solid instead of liquid triglycerides (9) this does not necessarily lead to slow release of drugs (10). In order to rationally design lipid nanoparticles as colloidal carrier drug delivery systems and to obtain information on their potential *in vivo* performance, it is thus necessary to fully characterize their drug retention and release properties. For this purpose, effective *in vitro* assays have to be established.

Many methods have been described to investigate the *in vitro* drug release from colloidal drug delivery systems such as sample and separate methods (11–13), dialysis based assays (3, 14, 15), continuous-flow methods (16, 17), and *in situ* techniques (8). Not all of them appear suitable to obtain undistorted information on the release of lipophilic drugs into a large volume of release medium (11, 17). Moreover, simple aqueous solutions that are often used as release media poorly reflect the *in vivo* situation such as intravenous administration. As a closer approach to the *in vivo* situation, the release medium can be supplemented with lipophilic particles like liposomes or emulsion droplets and the drug transfer into these particles be studied (10, 18, 19).

This study was aimed at comparing two of these transfer techniques with regard to their suitability to study the drug release behavior of differently structured lipid nanoparticles. The first technique utilized multilamellar vesicles (MLVs) containing 300 mM sucrose solution as "acceptors" for the drug released (19). In this setup, the donor and acceptor particles could be separated by centrifugation and the amount

[1] Department of Pharmaceutics and Industrial Pharmacy, Faculty of Pharmacy, Helwan University, Cairo, Egypt.
[2] To whom correspondence should be addressed. (e-mail: mohameddawoud2013@hotmail.com)

of drug transferred to the MLV is determined in the resulting MLV pellet. The second technique relied on the ability of flow cytometry to specifically detect fluorescent substances within sufficiently large acceptor particles. As in a recently proposed setup, donor nanoparticles were mixed with micrometer-sized emulsion droplets and the drug content in the acceptor droplets was analyzed *in situ* after dilution without any separation of donor and acceptor particles (10). To obtain additional information on a potential influence of the type of acceptor particles on the transfer profile, the two types of acceptor particles were tested in both transfer setups. Since the flow cytometric technique requires the use of fluorescent substances, a lipophilic temoporfin and the fluorescent dye Nile red (which differ in lipophilicity) were employed as model substances to investigate the transfer behavior. These drug models were incorporated into trimyristin nanoparticles which served as donor particles. Trimyristin nanoparticles can exist in two different physical states, depending on storage conditions after preparation by melt homogenization. After cooling to room temperature, the nanoparticles are present in the form of emulsion droplets in the supercooled liquid state whereas storage at lower temperatures, *e.g.,* in a refrigerator, will lead to crystallization of the matrix lipid and the formation of platelet-like structures (9, 20). This special property of trimyristin nanoparticles was utilized to additionally study the effect of the physical state of the donor particles on the transfer behavior.

MATERIALS AND METHODS

Materials

The triglyceride trimyristin (D114, Dynasan 114) and Miglyol 812 were a gift of Condea Chemie (Witten, Germany), partially hydrolyzed poly (vinyl alcohol) (PVA; Mowiol 3-83) was from Clariant (Frankfurt/Main, Germany), sodium glycocholate (SGC), cholesterol, Trizma 7.4 pre-set crystals, sucrose, praseodym (III)-chloride ($PrCl_3$), and sodium azide were from Sigma-Aldrich (Steinheim, Germany), egg phosphatidyl choline (EPC) and Lipoid S75 (S75) were obtained from Lipoid GmbH (Ludwigshafen, Germany), Nile red was obtained from Acros Organics (Geel, Belgium), temoporfin (5,10,15,20-tetrakis (3-hydroxyphenyl) chlorin) was a kind gift from Biolitec AG, Jena, Germany, glycerol from Solvay GmbH (Rheinberg, Germany), thiomersal from Caesar and Loretz (Hilden, Germany), methanol and tris were from Carl Roth GmbH (Karlsruhe, Germany), acetonitrile, ethanol, and chloroform all from VWR International (Darmstadt, Germany), tetrahydrofurane (THF) was from Fisher Scientific (Nidderau, Germany), and Hepes from AppliChem GmbH (Darmstadt, Germany). Purified water was prepared by filtration and deionization/reverse osmosis (Milli RX 20, Millipore, Schwalbach, Germany).

Methods

Preparation of Trimyristin Donor Lipid Nanoparticles

The dispersions were prepared from 5% (*w*/*w*) trimyristin stabilized with 1.8% (*w*/*w*) Lipoid S75 and 0.45% (*w*/*w*) sodium glycocholate (SGC) in an aqueous phase containing 2.25% glycerol for isotonization and 0.01% thiomersal for preservation. The preparation was done by high-pressure melt homogenization using a Microfluidizer M-110S (Microfluidics, Newton, MA, USA) (21). S75 and SGC were dispersed/dissolved in the aqueous phase by magnetic stirring overnight. The matrix lipid and the surfactant-containing aqueous phase were heated to 70°C. After melting of the triglyceride, the aqueous phase was poured to the molten lipid and the mixture was pre-homogenized for 1 min (Ultra-Turrax T8, IKA Labortechnic, Germany). This crude emulsion was transferred to the warm (70°C) high-pressure homogenizer and treated for 5 min at 500 bar. The resulting hot colloidal emulsion was allowed to cool to room temperature. Under these conditions, the matrix lipid remains in its liquid state due to supercooling (20).

To separate the solid trimyristin nanoparticles from the excess emulsifier S75, 5 ml samples of the nanosuspensions were subjected to ultracentrifugation (XL-80 ultracentrifuge, rotor type SW55 Ti, Beckman Coulter Inc., Fullerton, CA, USA) for 1 h at 35,000 rpm and 15°C. After removing the aqueous supernatant containing the excess emulsifiers, the pellet was scraped from the tube bottom, resuspended in 5 ml of surfactant-free aqueous phase and sonicated for 10 min at 60°C.

Loading with temoporfin (0.5 mg/ml) was carried out to the original nanoemulsion (before cooling and crystallization). A stock solution from temoporfin was prepared in methanol (10 mg/ml) and from this stock solution 500 µl was added to 10 ml of the nanoemulsion. Shaking of the samples was done for 2 days at 25°C in a shaking water bath (Grant OLS 200, Cambridge, England) followed by solidification and ultracentrifugation as described above. Loading of Nile red (0.15 mg/ml) was carried out by evaporation of an ethanolic dye stock solution (0.75 mg/ml) in a glass vial leaving behind a thin film of Nile red followed by addition of 5 ml from the resuspended nanoemulsion (after ultracentrifugation) and shaking at 25°C for 2 days followed by solidification of the nanoparticles in the refrigerator.

Preparation of the Acceptor Multilamellar Vesicles

The MLV liposomes were prepared as described before (19) but with slight modification in the molar ratio between EPC and cholesterol. One milliliter EPC chloroform stock solution (76 mg) was added to 1 ml cholesterol chloroform stock solution (9.68 mg) in a small bottom flask (EPC:cholesterol 8:2 mol/mol). The lipid mixture was dried to a thin film under vacuum (200 mbar for 2 h followed by 30 mbar for 1 h (Büchi Rotavapor R-114, Essen, Germany)). The resulting thin film was hydrated with 1 ml warm 300 mM sucrose solution under vortexing to yield MLV liposomes, which were transferred to a plastic Eppendorf tube. The mixture was centrifuged at 1,600×*g* for 10 min. After centrifugation, the MLV appeared as supernatant layer with the sucrose solution below. An 18G needle syringe was used to pierce the Eppendorf tube and to withdraw the sucrose solution. 0.5 ml of HBS pH 7.4 (20 mM Hepes, 150 mM NaCl adjusted to pH 7.4 with 1 M NaOH) was added to the remaining MLV. The sample was vortexed and centrifuged at 1,600×*g* for 10 min, after that the MLV appeared as a pellet (due to the presence of sucrose solution in their core). The HBS

supernatant was decanted and the pellet was washed twice with 0.5 ml HBS. The pellet was finally resuspended in fresh HBS (1 ml) and stored at refrigerator temperature. The procedure yielded MLV dispersions with a mean particle size around 11 μm (Fig. 1).

Preparation of the Acceptor o/w Emulsion Droplets

The acceptor oil/water (o/w) emulsion was composed of 5% (*w*/*w*) liquid medium chain triglycerides (Miglyol 812) stabilized with 3% (*w*/*w*) polyvinyl alcohol in an aqueous phase containing 2.25% glycerol and 0.01% thiomersal. The emulsion was prepared at room temperature using an Ultra-Turrax (T8, IKA Labortechnic, Germany) for 15 min. Emulsions with a mean particle size around 6 μm were obtained by this way (Fig. 1). The emulsion was stored at room temperature and used directly after preparation. For calibration of the flow cytometer, small fractions of the emulsions were loaded with different amounts of the investigated fluorescent dyes in the same way as described for the donor lipid nanoparticles.

Particle Size Analysis

Particle sizes of the donor lipid nanoparticles with and without the different drug models were measured by photon correlation spectroscopy (PCS) using a Zetasizer Nano ZS (Malvern Instruments Ltd., Worcestershire, UK). The dispersions were diluted with filtered demineralized water and measured at 25°C at a scattering angle of 173°. The results of three consecutive measurements of 5 min duration performed after 5 min of equilibration were averaged. The results are given as the *z*-average diameter and the polydispersity index (PDI, measure for the relative width of the particle size distribution).

The particle sizes of the donor nanoparticles before and after ultracentrifugation, the acceptor o/w emulsion droplets and MLV particles were measured with laser diffraction (LD) in combination with PIDS (polarization intensity differential scattering) using a Coulter LS 230 Particle Sizer (Beckman Coulter, Krefeld, Germany). Eight consecutive measurements of 90 s were averaged. The applied evaluation model used the Mie theory with a refractive index of 1.332 for water and 1.45 for the sample. The volume distributions of the samples were calculated and the results are given as the mean particle sizes.

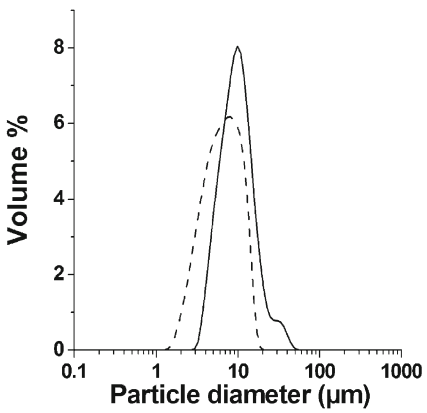

Fig. 1. LD-PIDS particle size distribution of the acceptor MLV and emulsion; *continuous line* MLV; *dashed line* emulsion. Note: these particle size distributions were only representative one as several batches of emulsion and MLV were prepared

Cryo-Transmission Electron Microscopy

A few microliters of the original nanoparticles (solidified particles before ultracentrifugation), resuspended nanoparticles (after ultracentrifugation) and liposomal layer (supernatant) were placed on a holey grid (Quantifoil Micro Tools, Jena, Germany) and excess of liquid was removed with filter paper (the samples were used without dilution). The samples were cryofixed by rapid immersing into liquid ethane cooled to −170 to −180°C in a cryobox (Carl Zeiss NTS GmbH, Oberkochen, Germany). Excess ethane was removed by blotting in the cold. The samples were transferred with a cryotransfer unit (Gatan 626-DH) into the pre-cooled cryoelectron microscope (Philips CM120, Netherlands) operated at 120 kV and viewed under low dose conditions.

^{31}P-Spectroscopy for the Donor Particles

In order to investigate the existence of liposomes (small unilamellar vesicles) due to the presence of excess S75 in addition to the triglyceride nanoparticles, ^{31}P-NMR spectroscopy was carried out for the nanoparticles before and after ultracentrifugation and for the supernatant layer (excess S75) (22–24). The samples (500 μl) were analyzed by high-resolution ^{31}P nuclear magnetic resonance (NMR) in a Bruker Avance 400 apparatus (Bruker, Karlsruhe, Germany) operating at 30°C before and after the addition of an aqueous praseodymium chloride ($PrCl_3$) solution (1 mg/ml). Deuterium oxide (D_2O) was used as an external reference in a Wilmad NMR reference tube (2 mm), which was placed inside a 5-mm NMR sample tube containing the sample. In the paramagnetic-shifted samples, praseodymium chloride solution was added in 1:5 (*v*/*v*) portions (100 μl praseodymium chloride and 400 μl sample).

Determination of the Lipid Content of the Donor Trimyristin Nanoparticles by HPLC

The amount of matrix lipid in the nanoparticles before and after ultracentrifugation and supernatant layer was determined using reversed phase HPLC with evaporative light scattering detection (Varex MKIII ELSD, Alltech GmbH, Unterhaching, Germany). The analysis was performed with a 25 cm×3 mm LiChrocart column packed with LiChrospher 100-5 RP 18 (Merck KgaA, Darmstadt, Germany) in a System Gold 126 HPLC (Beckman Coulter GmbH, Krefeld, Germany). Acetonitrile-tetrahydrofurane 55:45 (*v*/*v*) was used as the mobile phase and the isocratic flow rate was set at 1 ml/min. For the evaporation of the mobile phase, the temperature of the detector was adjusted at 91°C and the pressure of nitrogen gas was 2.2 L/min. A calibration curve for trimyristin was obtained from measurements of standard solutions of trimyristin. To determine the amount of trimyristin in the nanoparticles, small amounts of the nanoparticle dispersions (before and after ultracentrifugation) and supernatant layers were dissolved in acetonitrile-tetrahydrofurane 20:80 (*v*/*v*) to prepare 1 μl/ml samples and 100 μl of these solutions were

injected into the HPLC for analysis. The amount of trimyristin in the samples was determined from the calibration curve.

Temoporfin Content

Since temoporfin was added to the D114 formulations before solidification and ultracentrifugation some drug was lost into the supernatant layer (excess S75) after ultracentrifugation. The amount of the drug in 20 μl ultracentrifuged and resuspended nanoparticles (pellets) and supernatant layer was determined after diluting the samples to 5 ml with a mixture of acetonitrile-tetrahydrofurane 20:80 (*v*/*v*) and measuring the UV absorbance at 421 nm.

Transfer Investigations with the Centrifugation Technique

Transfer to the Acceptor Multilamellar Vesicles. Transfer of temoporfin was studied from the donor resuspended nanoparticles in the liquid form, which was prepared by melting the crystalline form (at 60°C), to the acceptor MLV particles. Different amounts of the donor were added to Eppendorf tubes containing 600 μl of the acceptor MLV and different amounts of HBS (the total volume was 1 ml). The samples were incubated in a shaking water bath at 37°C. Samples were taken at specific times, vortexed and centrifuged (3MK centrifuge, Sigma, Osterode, Germany) at 5,300 rpm (1,600×*g*) for 10 min to separate the nanoparticles from the pellet MLV liposomes. The supernatant (nanoparticles) was collected by decantation and absorbance was measured at 421 nm after dilution with a mixture of acetonitrile-tetrahydrofurane 20:80 (*v*/*v*) to 5 ml. The MLV-containing pellet was washed twice with 250 μl HBS, vortexed, and centrifuged (the centrifugation time for each washing was 10 min). The first and second washings were combined and the absorbance was measured at 421 nm after dilution with the same solvent mixture to 5 ml. The amount of drug detected in the supernatant and washes was combined to obtain an overall supernatant amount from which the percent drug retained in the nanoparticles was determined. The amount of the drug in the MLV (percent drug transferred) was determined by dissolving the MLV pellets in ethanol, diluting to 5 ml and measuring UV absorbance at 421 nm. The temoporfin recovery was calculated from the percentage of drug transferred and retained.

The transfer of Nile red from the resuspended liquid nanoparticles to the acceptor MLV was studied with a molar ratio of 1:100. Donor particles (15 μl) were added to Eppendorf tubes, which contained 385 μl HBS and 600 μl MLV. The transfer procedures were done as described before with temoporfin and the UV absorbance was measured at 548 nm.

Transfer to the Acceptor o/w Emulsion. The transfer of temoporfin from the resuspended crystalline nanoparticles to the acceptor o/w emulsion was studied with a molar ratio of 1:25. Different amounts of the crystalline loaded donor particles were mixed with 1 ml of the acceptor o/w emulsion in Eppendorf tubes. The Eppendorf tubes were incubated in a shaking water bath at 37°C (Grant OLS 200, Cambridge, England). After incubation, the samples were diluted with 3-ml purified water into an ultracentrifugation tube. The samples were ultracentrifuged (XL-80 ultracentrifuge, rotor type SW55 Ti, Beckman Coulter Inc., Fullerton, CA, USA) for 30 min at 55,000 rpm. After removing the cream layer (containing the emulsion) and aqueous supernatant, the pellet (containing the trimyristin nanoparticles) was scraped from the tube bottom, resuspended in 250 μl of water and sonicated for 2 min. The suspension was transferred into glass vials and the centrifugation tube was rinsed with 250 μl water, which was added to the glass vials. The pellet suspension was dissolved in 3 ml of a mixture of acetonitrile-tetrahydrofurane 20:80 (*v*/*v*) and the UV absorbance was measured at 421 nm. The transfer of Nile red to the acceptor o/w emulsion was studied in the same way as for temoporfin but with a molar ratio of 1:100 where 20 μl of the donor particles was mixed with 1 ml of the acceptor emulsion in Eppendorf tubes and the UV absorbance of was measured at 548 nm.

Transfer Investigations by Flow Cytometry

General Procedure. The measurements were performed in a similar way as described previously (10). To select the conditions for the fluorescence measurements, the acceptor particles were measured (without drug) in the flow cytometer. Different amounts of the acceptor dispersions were diluted with purified water in a measurement tube and subsequently measured by flow cytometry. The right amount of the acceptors was achieved when a count rate of approximately 250 events per second was reached. After the detection of 10,000 events the measurements were stopped. The emitted fluorescence of temoporfin and Nile red was detected at the photomultiplier tube number 4 (FL4) with a wavelength range of 665–685 nm. The flow cytometer was calibrated by measuring the fluorescence intensity of acceptor samples, which had been loaded with defined amounts of the drug models, and the fractions of drug transferred were calculated from these calibration curves. Between the measurements, cleaning steps were introduced to avoid mixing with residual particles of preceding samples.

Transfer to the Acceptor MLV and o/w Emulsion. The transfer of temoporfin and Nile red was investigated by mixing different amounts of the loaded donor particles with 1 ml of the acceptor o/w emulsion or 600 μl of the acceptor MLV in Eppendorf tubes. The tubes were subsequently incubated in a water bath shaker at 37°C (Grant OLS 200, Cambridge, England). Samples were collected at different time points after mixing; 5 and 12 μl of the transfer mixture in case of the acceptor MLV and emulsion, respectively, were diluted in 1-ml purified water and subsequently measured at the flow cytometer.

Transfer Kinetics. The transfer curves of the percent transferred amount of temoporfin and Nile red to the different acceptor particles using the two transfer techniques were exponentially fitted using Microcal Origin 6.0 software (OriginLab Corporation, Northampton, MA, USA) and the exponential function:

$$A_{acc} = A_{final} - A \times e^{-k \times t} \quad (1)$$

A_{acc} is the amount in percent of drug transferred to the acceptor particles at time t, A_{final} is the final transferred amount in percent of drug and marks the height of the plateau, A is a pre-exponential coefficient and k is the rate constant of the transfer. The equilibrium time was determined by calculating the time required to reach 99% of the equilibrium amount.

RESULTS

Preparation of the Donor Nanoparticles

The basic donor formulations were prepared by high-pressure homogenization resulting in dispersions with PCS z-average values around or slightly above 100 nm (Table I). For trimyristin nanoparticles crystallized by storage at refrigerator temperature slightly larger particle sizes were observed than for the corresponding emulsion formulations (stored at room temperature). This effect can be attributed to a change in particle shape during recrystallization of the nanoparticles. The spherical emulsion droplets transform into platelet-shape crystals with a larger hydrodynamic PCS diameter (20). The particle size of nanoparticles loaded with the drug models was similar to that of their unloaded counterparts (Table I).

After high-pressure homogenization, colloidal lipid emulsions and suspensions of solid lipid nanoparticles stabilized with the aid of phospholipids may contain a significant fraction of small unilamellar vesicles (SUV) that are formed by excess phospholipids (23, 25–27). Since the drug transfer experiments were intended to provide information on the behavior of drugs associated with triglyceride nanoparticles (not with vesicles) an ultracentrifugation step was carried out on the crystallized nanoparticles to separate them from excess phospholipids. Similar procedures are often used in the investigation of parenteral fat emulsions (22–24). After the centrifugation step, fractions of the dispersions were heated to melt the resuspended crystalline nanoparticles and to obtain corresponding trimyristin emulsions for comparative investigations.

Effect of Ultracentrifugation on the Properties of the Donor Nanoparticles

A series of characterization experiments was carried out in order to check the success of the ultracentrifugation procedure (*i.e.*, complete separation of the excess phospholipid vesicles) and to rule out negative effects on the colloidal quality of the donor nanoparticles due to the stress of centrifugation.

Particle Size Distribution

A certain effect of the ultracentrifugation procedure on the particle size distribution had to be expected since the vesicular fraction typically contains comparatively small particles that are removed into the supernatant. Moreover, the mechanical stress upon ultracentrifugation might lead to an aggregation of the triglyceride nanoparticles. Compared to that of the non-centrifuged dispersions, the PCS z-average values of the crystalline nanoparticles had indeed increased after ultracentrifugation and redispersion but the PDI values all remained far below 0.2 indicating an acceptable homogeneity of the particle size distributions (Table I). A slight shift to larger particle size values was confirmed by laser diffractometry (LD) in combination with polarization intensity differential scattering (PIDS) (Fig. 2).

Cryo-Transmission Electron Microscopy

Nanoparticles were investigated by cryo-transmission electron microscopy (cryo-TEM) to check for effects of the ultracentrifugation procedure (Fig. 3). In this figure, weak circular and ellipsoidal structures, which represent the thin trimyristin platelets in top view, can be recognized. If the particles are viewed edge-on, they appear as dark rods or needles since, in this position, the increased thickness of the structures leads to a darker appearance (25). The presence of these structures could be observed in all dispersions under investigation, including the supernatant layer. A small amount of phospholipid vesicles could be observed in the images of the supernatant layer (Fig. 3c) where they appeared as small ring-shaped structures. These liposomal structures could not, however, be observed in the images of resuspended nanoparticles after ultracentrifugation and the original lipid nanoparticles (before ultracentrifugation). In case of the original nanoparticles, the liposomal structures may not be observable due to the abundance of the crystalline nanoparticles in the medium. In the images of the resuspended nanoparticles, the lack of these liposomal structures might be correlated with their removal by the ultracentrifugation process.

^{31}P-NMR Spectroscopy

^{31}P-NMR spectroscopy was used to confirm the presence of liposomes due to the excess S75 in the nanoparticle

Table I. PCS z-Average Mean Particle size and Polydispersity Indices (PDI) of the Trimyristin Nanoparticles (Before and After Ultracentrifugation)

	z-Average ± SD/PDI			
	Unloaded			
Formulation	Stored at 23°C	Stored at 4°C	Loaded with temoporfin	Loaded with Nile red
Nanoparticles before ultracentrifugation	115±0.6/0.14	122±0.7/0.16	123±0.9/0.17	
Nanoparticles after ultracentrifugation		141±0.4/0.11	142±1.5/0.11	148±1 nm/0.19

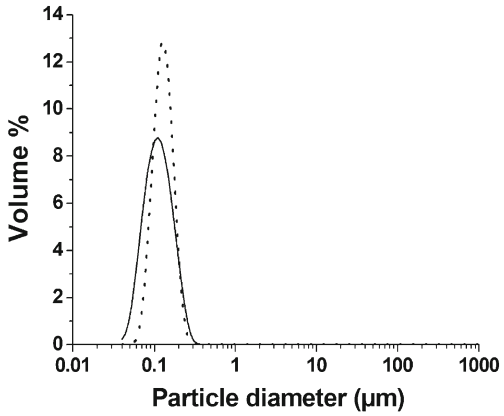

Fig. 2. LD-PIDS particle size distribution of the crystalline lipid nanoparticles; *continuous line* original lipid nanoparticles before ultracentrifugation; *dashed line* resuspended nanoparticles after ultracentrifugation

dispersions and to determine the distribution of the phospholipid between the triglyceride nanoparticles and the liposomes. Furthermore, NMR spectroscopy was performed to ensure that the excess S75 liposomes were separated from the lipid nanoparticles by the ultracentrifugation process. Figure 4 shows the NMR spectra of original nanoparticles before ultracentrifugation, resuspended nanoparticles and supernatant layer. Two signals with different line shapes can be observed in the original dispersion (Fig. 4a). A larger and sharper signal (around 0 ppm) was attributed to phospholipid headgroups in a more hydrophilic environment (liposomes formed by the excess S75) (23). The broader zone of resonance was attributed to the phospholipid headgroups in a more lipophilic environment, which belong to the phospholipid coat of the trimyristin nanoparticles (23). The sharp signal, which represents the phospholipid of the liposomes, was lost after centrifugation and only the broader signal (the phospholipid coat of the trimyristin nanoparticles) remained in the resuspended nanoparticles (Fig. 4c). Both signals (the sharp and the broad one) were observed in the supernatant layer after ultracentrifugation, which indicates the presence of the two populations of the phospholipid (phospholipid coat of the triglyceride particles and phospholipid in liposomes due to the excess S75) (Fig. 4e). To confirm the assignment of the two signals, praseodymium chloride ($PrCl_3$) was added to the different dispersions as a shifting reagent. $PrCl_3$ only interferes with the accessible phospholipid (phospholipid of the outer liposomes layer and phospholipid coat of the triglyceride nanoparticles) but not with the inner phospholipid layer of liposomes (23, 24). The sharp signal was still present in the case of the original formulations before ultracentrifugation but with a smaller intensity than without $PrCl_3$ (Fig. 4b). This decrease in intensity was due to the shift of the signal of the accessible phospholipid headgroups leaving only the signal of the inaccessible phospholipid headgroups belonging to the inner phospholipid layer of liposomes at the original position. The broad peak was shifted to about 10 ppm. Corresponding results were obtained with the supernatant layer after the ultracentrifugation process, which indicates the presence of triglyceride nanoparticles as well as liposomes in this supernatant layer (Fig. 4f). In case of the resuspended nanoparticles, the broad peak related to the phospholipid coat of the triglyceride nanoparticles was shifted to about 15 ppm (Fig. 4d). The results obtained after addition of $PrCl_3$ thus confirm the conclusions drawn from the original spectra and that the excess S75 liposomes were removed by the ultracentrifugation step.

High-Performance Liquid Chromatography of the Donor Particles

Since the ultracentrifugation process may lead to a loss of triglyceride from the formulations, a determination of the real triglyceride content in the nanoparticle before and after ultracentrifugation was performed by HPLC. Only 77% of the original trimyristin content remained in the redispersed nanoparticle suspensions after ultracentrifugation. About 20% of the trimyristin was lost into the supernatant during the ultracentrifugation process.

Temoporfin Content

About 35% ± 1.5 and 66% ± 2.1 temoporfin were observed in nanoparticles after ultracentrifugation and the corresponding supernatant layers, respectively. According to these results, the drug affinity is higher for liposomes (the supernatant layer) than for the resuspended lipid nanoparticles. It has been reported earlier that crystalline lipid

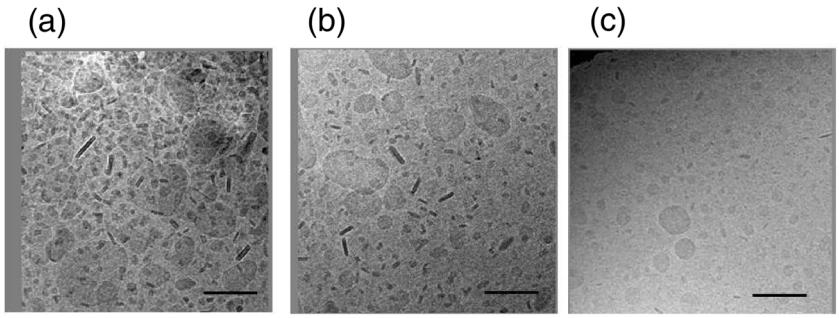

Fig. 3. Cryo-TEM images of the crystalline lipid nanoparticles; **a** original nanoparticles before ultracentrifugation; **b** resuspended nanoparticles after ultracentrifugation; **c** supernatant layer; the *bar* represents 200 nm

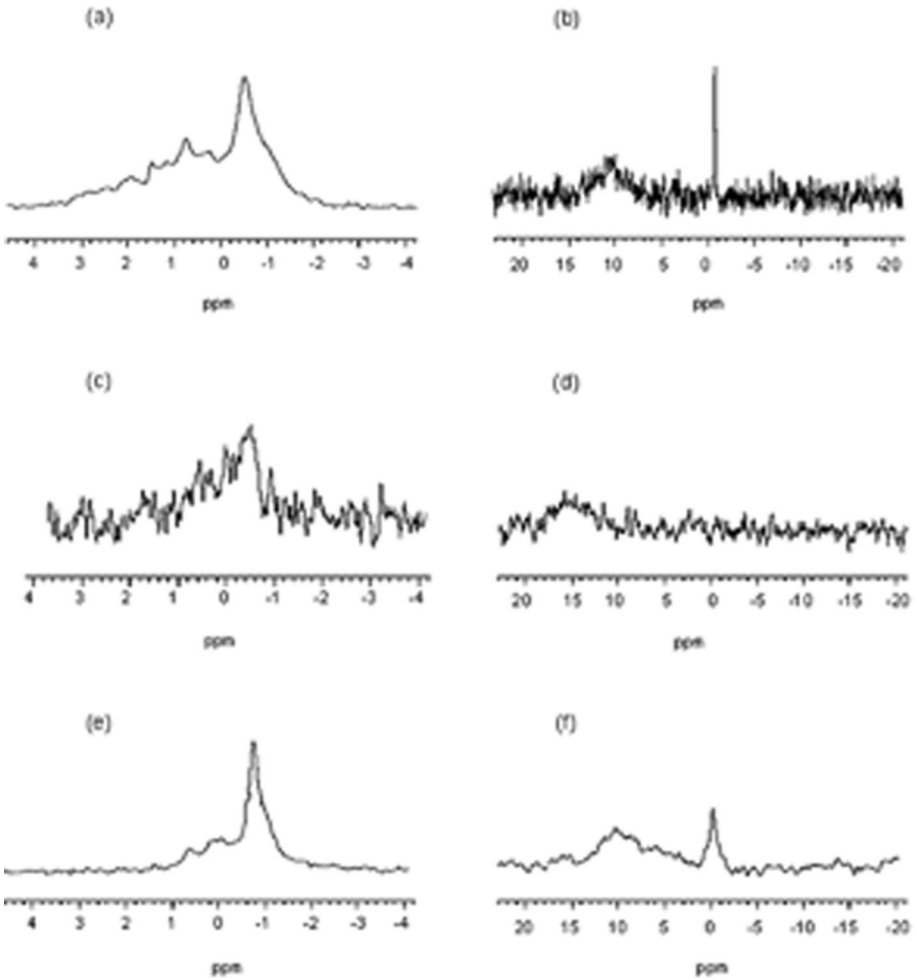

Fig. 4. ^{31}P-NMR spectra of the crystalline lipid nanoparticles; **a** original nanoparticles before ultracentrifugation without $PrCl_3$; **b** original nanoparticles before ultracentrifugation with $PrCl_3$; **c** resuspended nanoparticles without $PrCl_3$; **d** resuspended nanoparticles with $PrCl_3$; **e** supernatant layer without $PrCl_3$; **f** supernatant layer with $PrCl_3$

nanoparticles exhibit a low drug payload capacity and drug expulsion into the aqueous phase may occur due to the transition into highly ordered lipid particles during lipid crystallization (9, 27–29). As observed in the ^{31}P-NMR spectroscopy, cryo-TEM and the HPLC analysis of the supernatant layer, which contains the excess emulsifier S75, this supernatant layer also, contains a certain amount of D114 crystalline nanoparticles and this may increase the drug content in the liposomal layers.

Investigation of Dye Transfer Using the Two Techniques. Transfer experiments using the centrifugation method with the acceptor MLV can be performed only with liquid donor nanoparticles and not with crystalline nanoparticles while with the acceptor emulsion the crystalline donor nanoparticles should be used to achieve adequate separation. The flow cytometric technique was used to monitor the drug transfer from lipid donor particles in crystalline or liquid form to the acceptor MLV and emulsion as the particle size of both acceptors (about 11 and 6 μm for the MLV and emulsion, respectively) was large enough to be recognized by the flow cytometer (10). Moreover, the lower size detection limit of 0.5 μm indicates that a detection of the donor lipid nanoparticles with a z-average diameter below 0.2 μm will not be possible and thus that these small particles will not disturb the measurements (10).

Transfer of Temoporfin to the Acceptor MLV and Emulsion

The transfer of temoporfin to the acceptor MLV was moderate as determined with the centrifugation technique for different donor:acceptor ratios (Fig. 5); *e.g.*, for a molar ratio of 1:100, the amount of temoporfin transferred after 0.5 h was 23. The steady state concentration was reached after about 12 h at a molar ratio of 1:25 while the equilibrium was obtained after about 11 and 10 h at molar ratios of 1:50 and 1:100, respectively (Table II). The transfer rate constant ranged from 0.005 to 0.0065 min^{-1} with the different molar ratios. While transfer rate constant and time to equilibrium were only little affected by the molar ratio, the final amount of temoporfin transferred increased with increasing concentration of acceptor particles as expected. With the centrifugation method, it was also possible to

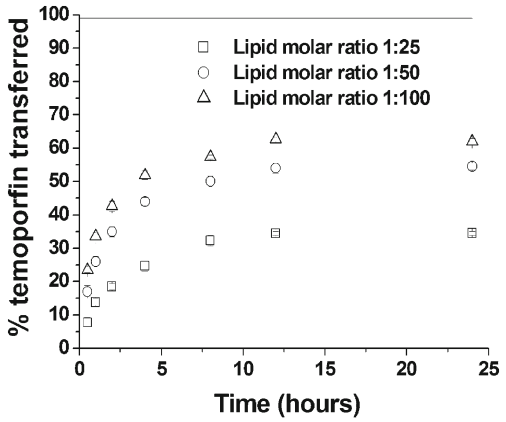

Fig. 5. Transfer of temoporfin from the resuspended lipid nanoparticles in the liquid form to the acceptor MLV as determined by the centrifugation technique at different time intervals; *continuous line* equal distribution of temoporfin between the donor and acceptor particles

determine the fraction of temoporfin that was retained in the nanoparticles at different time points. The recovery of temoporfin (total of percentage transferred and retained) ranged between 95% and 103%.

Temoporfin transfer from resuspended crystalline nanoparticles to the acceptor o/w emulsion was measured after separating the donor and acceptor by ultracentrifugation. Contrary to the acceptor MLV, the drug transfer to the acceptor emulsion was very rapid and equilibrium was obtained after about 3 min (Fig. 6, Table II). After 30 s the drug transfer was about 20% and at equilibrium about 33% had been transferred. Although the final percentage of temoporfin transferred to the acceptor emulsion was nearly the same as with the acceptor MLV (at the same donor: acceptor molar ratio), the transfer rate constant with the acceptor emulsion was much higher (Table II).

Since centrifugation experiments with MLV and emulsion droplets as acceptor particles had to be carried out with different physical states of the donor particles the flow cytometric technique was used to check for potential influences of this fact. Moreover, this technique has a very good time resolution and allows following rapid transfer processes more reliably than the centrifugation technique. With the flow cytometric technique, the transfer of temoporfin to the acceptor emulsion showed nearly the same equilibrium values that were observed with the centrifugation technique (Fig. 7) but the transfer rate constant was a bit lower than with the centrifugation technique (Table II) indicating a slight overestimation of the transfer rate determined with the centrifugation technique.

With both acceptors and transfer detection techniques, the final amount of temoporfin transferred was much lower than the expected equilibrium values. Assuming an equal temoporfin distribution between the donor and acceptor, about 99% of the temoporfin was expected in the different acceptors at a molar ratio of 1:100 between the donor and acceptor and about 96% at a molar ratio of 1:25. However, the experimentally determined amount of transferred temoporfin ranged only between 35% and 70% (Table II).

Nile red Transfer to the Acceptor MLV and Emulsion

In order to study the effect of lipophilicity on the transfer, Nile red, which is less lipophilic than temoporfin, was used as a drug model. The transfer of Nile red from the resuspended lipid nanoparticles in the liquid or crystalline form to the acceptor MLV and emulsion was investigated with the centrifugation technique and a molar ratio of 1:100. The liquid nanoparticles were used with the acceptor MLV while the crystalline nanoparticles were used with the acceptor emulsion. In contrast to temoporfin transfer, the transfer of Nile red to both acceptors was very rapid (equilibration within about two minutes) and complete transferred amount of Nile red at equilibrium corresponded to the expected value (Figs. 8 and 9). With the flow cytometric method, the transfer of Nile red seemed to be completed after about 3 min with the

Table II. Kinetic Parameters Derived from Fits to the Transfer Curves of Temoporfin and Nile red from the Lipid Nanoparticles to the Different Acceptors Obtained by the Ultracentrifugation and Flow Cytometric Technique

Donor	Acceptor	Molar ratio	Transfer rate constant K (min^{-1})	Final% transferred	Equilibrium time
Ultracentrifugation technique					
Nanoemulsion (temoporfin)	MLV	1:25	0.005±0.0005	35±2.1	12.5 h
		1:50	0.0065±0.001	53±1.2	10.8 h
		1:100	0.0065±0.0007	61±1.7	10 h
Crystalline nanoparticles (temoporfin)	o/w emulsion	1:25	1.28±0.15	32±0.8	3 min
Nanoparticles (Nile red)[a]	MLV	1:100	1.9±0.08	98±1.8	2 min
	o/w emulsion	1:100	3.3±0.37	101±1.9	1 min
flow cytometric technique					
Crystalline nanoparticles (temoporfin)	o/w emulsion	1:25	0.95±0.03	33±1.1	4.4 min
		1:50	0.85±0.04	47±0.9	5.4 min
		1:100	0.81±0.07	65±1.5	5.5 min
Nanoparticles (Nile red)[a]	MLV	1:100	1.05±0.07	100.5±1.5	3.8 min
	o/w emulsion	1:100	1.91±0.05	100±1.15	3 min

[a] Liquid lipid nanoparticles (nanoemulsion) with the acceptor MLV and crystalline lipid nanoparticles with the acceptor emulsion

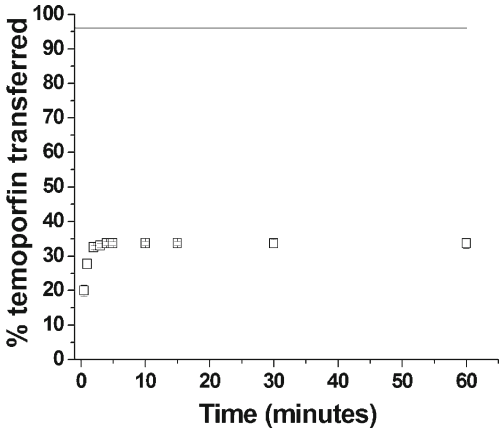

Fig. 6. Transfer of temoporfin from the resuspended crystalline nanoparticles to the acceptor o/w emulsion as determined by the centrifugation technique at different time intervals (molar ratio 1:25); *continuous line* equal distribution of temoporfin between the donor and acceptor particles

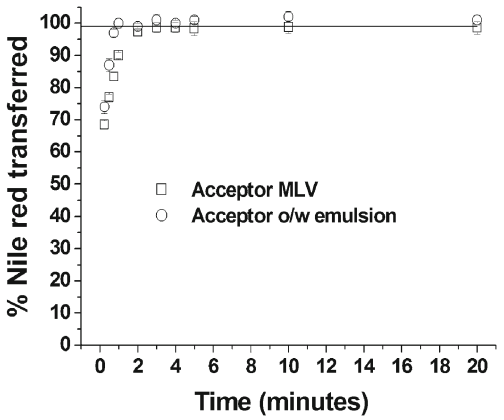

Fig. 8. Transfer of Nile red from the resuspended nanoparticles to the acceptor o/w emulsion and MLV with molar ratio 1:100 as determined by the centrifugation technique at different time intervals; *continuous line* equal distribution of Nile red between the donor and acceptor particles

different acceptors (Table II). Already after 1 min more than 75% of Nile red had been transferred with both acceptors. Accordingly, the transfer rate constant derived from the centrifugation technique (Table II) was slightly higher than the transfer rate constant obtained from the flow cytometric technique (Table II).

DISCUSSION

Many factors may affect drug transfer from donor particles to acceptor sites *in vitro* and *in vivo*. To obtain information on the factors that influence drug transfer two *in vitro* techniques were used to monitor the drug transfer from lipid nanoparticles to different types of acceptor particles that were intended to mimic lipophilic acceptor sites in the body. The centrifugation technique had certain limitations regarding the physical state of the donor nanoparticles. With MLV as acceptor particles, only liquid donor nanoparticles could be used to achieve adequate separation whereas crystalline donor nanoparticles were required to allow separation from the acceptor emulsion droplets. With the centrifugation method, it was thus impossible to measure the drug transfer from the crystalline and liquid donor nanoparticles to a single type of acceptor. Another disadvantage of the centrifugation technique, especially in situations that lead to rapid drug transfer, is its lower time resolution that can lead to an overestimation of the transfer rate constant. In contrast to the centrifugation technique, flow cytometry can be used with both types of the donor lipid nanoparticles (crystalline and liquid particles). Moreover, the high time resolution of this technique, which does not require separation of donor and acceptor particles, allowed to study the very rapid transfer of Nile red and temoporfin to the acceptor emulsion with good time resolution and to obtain many data points in the rising part of the transfer curve of these substances. A limiting factor for flow cytometry is the size of the acceptor particles, which should be in the lower micrometer range. Furthermore, the need for fluorescent substances is a severe restriction of possible candidates for investigation and limits the use of this method to model fluorescent substances.

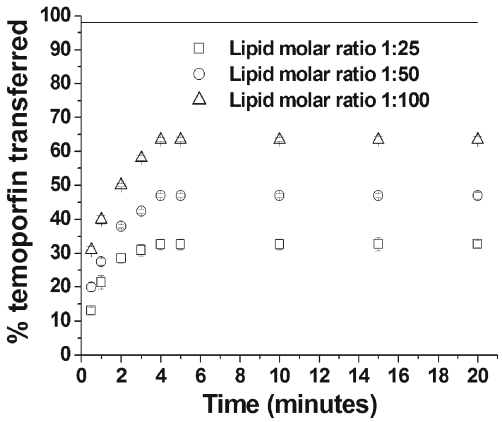

Fig. 7. Transfer of temoporfin from the resuspended crystalline nanoparticles to the acceptor o/w emulsion as determined by the flow cytometric technique at different time intervals; *continuous line* equal distribution of temoporfin between the donor and acceptor particles

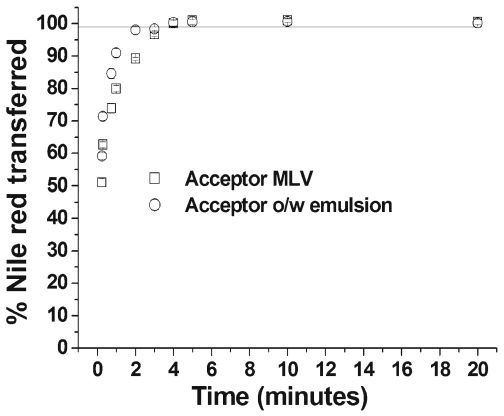

Fig. 9. Transfer of Nile red from the resuspended nanoparticles to the acceptor o/w emulsion and MLV with molar ratio 1:100 as determined by the flow cytometric technique at different time intervals; *Continuous line* equal distribution of Nile red between the donor and acceptor particles

The transfer of temoporfin from the donor lipid nanoparticles to the different acceptors was characterized by different rates depending on the acceptor used. The transfer to the acceptor MLV was characterized by a moderate rate whereas to the acceptor o/w emulsion the transfer was very rapid. For both acceptors, the transfer stopped at concentrations far below an equal distribution between the donor and acceptor. The low equilibrium value might be attributed to the location of temoporfin at the interface of the acceptor particles as a result of a certain amphiphilicity (30). Due to the limited size of the large acceptor particles, saturation might occur and thus probably the transfer stops at a low level as previously also assumed (10).

As mentioned above, the transfer rate to the acceptor MLV was much lower in comparison to that to the acceptor emulsion. The main reason for this large difference in the transfer rates may be the difference in the composition and particle size of the two acceptors. The acceptor MLV particles were composed of multilayers with mean particle size about 11 μm. On the contrary, the acceptor emulsion with a mean particle size of 6 μm was composed of homogenous single droplets. The difference in particle size means that a higher number of acceptor emulsion droplets were present in the transfer mixture than in the mixture with the acceptor MLV, which may have accelerated the transfer. Additionally, the acceptor MLV was prepared from EPC with cholesterol, which increases the rigidity of the bilayers and thus decreases the rate of temoporfin transfer from layer to layer within the MLV multilayer (31).

For both acceptors, an increase in the acceptor to donor ratio led to an increase in the final amount of temoporfin transferred. This observation was not unexpected and can simply be attributed to the increase in the number of the acceptor particles relative to the donor particles. The transfer rate constant did, however, not increase due to the increase in acceptor to donor ratio.

One of the most important factors, which exhibited a clear influence into the transfer behavior, was the lipophilicity of the drug. Nile red was used as alternative drug model with less lipophilic character than temoporfin where the log*P* of Nile red was about 3.5 and for temoporfin it was about 9 (10). The lower lipophilicity of Nile red allowed the fast diffusion of Nile red molecules to the different acceptor particles resulting in very rapid transfer. Also, the diffusion of Nile red from layer to layer within the MLV acceptor seems to have been easier as there were only slight differences in the transfer behavior to emulsion droplets and MLV particles. For both types of acceptor particles, a slightly higher transfer rate constant of Nile red was determined with the centrifugation techniques than with the flow cytometric technique. This confirms the conclusion from the experiments with temoporfin, that the higher time resolution of the flow cytometric technique makes it more suitable to monitor very rapid transfer process.

CONCLUSION

The centrifugation technique is suitable for measuring slow and moderate drug transfer processes whereas the flow cytometric method can also be used for more rapid transfer processes. Since flow cytometry relies on the detection of fluorescence, it will, however, not be applicable for most drugs.

Concerning the influence of the donor system, the results observed with the two techniques are in good agreement with previous studies (10) indicating that the lipophilicity of the drug model highly affects the transfer behavior period.

The course of the transfer process depends on several experimental factors such as the ratio of acceptor to donor particles. Moreover, the size, composition and structure of the acceptor particles seem to play a major role. In this study, MLV turned out to be less suitable acceptor particles than emulsion droplets. This influence of the type of acceptor particles needs to be carefully observed when selecting the experimental conditions for drug transfer studies.

REFERENCES

1. Elbaz E, Zeevi A, Klang S, Benita S. Positively charged submicron emulsions—a new-type of colloidal drug carrier. Int J Pharm. 1993;96:R1–6.
2. Levy MY, Benita S. Design and characterization of a submicronized o/w emulsion of diazepam for parenteral use. Int J Pharm. 1989;54:103–12.
3. Levy MY, Benita S. Drug release from submicronized o/w emulsion—a new in vitro kinetic evaluation model. Int J Pharm. 1990;66:29–37.
4. Venkataram S, Awini WM, Jordan K, Rahman YE. Pharmacokinetics of 2 alternative dosage forms for cyclosporine—liposomes and intralipid. J Pharm Sci. 1990;79:216–9.
5. Lundberg BB, Risovic V, Ramaswamy M, Wasan KM. A lipophilic paclitaxel derivative incorporated in a lipid emulsion for parenteral administration. J Control Release. 2003;86:93–100.
6. Magenheim B, Levy MY, Benita S. A new in-vitro technique for the evaluation of drug-release profile from colloidal carriers - ultrafiltration technique at low-pressure. Int J Pharm. 1993;94:115–23.
7. Takino T, Konishi K, Takakura Y, Hashida M. Long circulating emulsion carrier systems for highly lipophilic drugs. Biol Pharm Bull. 1994;17:121–5.
8. Washington C, Evans K. Release rate measurements of model hydrophobic solutes from submicron triglyceride emulsion. J Control Release. 1995;33:383–90.
9. Westesen K, Bunjes H, Koch MHJ. Physicochemical characterization of lipid nanoparticles and evaluation of their drug loading capacity and sustained release potential. J Control Release. 1997;48:223–36.
10. Petersen S, Fahr A, Bunjes H. Flow cytometry as a new approach to investigate drug transfer between lipid particles. Mol Pharm. 2010;7:350–63.
11. Boyd BJ. Characterisation of drug release from cubosomes using the pressure ultrafiltration method. Int J Pharm. 2003;260:239–47.
12. Cui F, Shi K, Zhang LQ, Tao AJ, Kawashima Y. Biodegradable nanoparticles loaded with insulin-phospholipid complex for oral delivery: Preparation, in vitro characterization and in vivo evaluation. J Control Release. 2006;114:242–50.
13. Hu FQ, Yuan H, Zhang HH, Fang M. Preparation of solid lipid nanoparticles with clobetasol propionate by a novel solvent diffusion method in aqueous system and physicochemical characterization. Int J Pharm. 2002;239:121–8.
14. D'Souza SS, DeLuca PP. Development of a dialysis in vitro release method for biodegradable microspheres. AAPS Pharmscitech. 2005;6:E323–E8.
15. Washington C. Drug release from microdisperse systems: a critical review. Int J Pharm. 1990;58:1–12.
16. D'Souza SS, DeLuca PP. Methods to assess in vitro drug release from injectable polymeric particulate systems. Pharm Res. 2006;23:460–74.
17. Washington C, Koosha F. Drug release from microparticulates—deconvolution of measurement errors. Int J Pharm. 1990;59:79–82.

18. Fahr A, van Hoogevest P, May S, Bergstrand N, Leigh MLS. Transfer of lipophilic drugs between liposomal membranes and biological interfaces: consequences for drug delivery. Eur J Pharm Sci. 2005;26:251–65.
19. Shabbits JA, Chiu GNC, Mayer LD. Development of an in vitro drug release assay that accurately predicts in vivo drug retention for liposome-based delivery systems. J Control Release. 2002;84:161–70.
20. Bunjes H, Westesen K, Koch MHJ. Crystallization tendency and polymorphic transitions in triglyceride nanoparticles. Int J Pharm. 1996;129:159–73.
21. Bunjes H, Koch MHJ. Saturated phospholipids promote crystallization but slow down polymorphic transitions in triglyceride nanoparticles. J Control Release. 2005;107:229–43.
22. Drew J, Liodakis A, Chan R, Du H, Sadek M, Brownlee R, *et al*. Preparation of lipid emulsions by pressure extrusion. Biochem Int. 1990;22:983–92.
23. Ferezou J, Lai NT, Leray C, Hajri T, Frey A, Cabaret Y, *et al*. Lipid-composition and structure of commercial parenteral emulsions. BBA Lipid Lipid Met. 1994;1213:149–58.
24. Rotenberg M, Rubin M, Bor A, Meyuhas D, Talmon Y, Lichtenberg D. Physicochemical characterization of intralipid emulsions. Biochim Biophys Acta. 1991;1086:265–72.
25. Westesen K, Siekmann B. Investigation of the gel formation of phospholipid-stabilized solid lipid nanoparticles. Int J Pharm. 1997;151:35–45.
26. Dawoud M. Investigations on the transfer of porphyrin from o/w emulsion droplets to liposomes with two different methods. Drug Dev Ind Pharm. 2013.
27. Dawoud M. Transfer of a lipophilic drug model from lipid nanoparticle carriers to a lipophilic acceptor compartment. Am J PharmTech Res. 2013;3:370–86.
28. Wissing SA, Kayser O, Müller RH. Solid lipid nanoparticles for parenteral drug delivery. Adv Drug Deliv Rev. 2004;56:1257–72.
29. zur Mühlen A, Schwarz C, Mehnert W. Solid lipid nanoparticles (sln) for controlled drug delivery - drug release and release mechanism. Eur J Pharm Biopharm. 1998;45:149–55.
30. Wiehe A, Shaker YM, Brandt JC, Mebs S, Senge MO. Lead structures for applications in photodynamic therapy. Part 1: synthesis and variation of m-thpc (temoporfin) related amphiphilic a(2)bc-type porphyrins. Tetrahedron. 2005;61:5535–64.
31. Liu XY, Yang Q, Kamo N, Miyake J. Effect of liposome type and membrane fluidity on drug-membrane partitioning analyzed by immobilized liposome chromatography. J Chromatogr A. 2001;913:123–31.